Pure appl. geophys. 155 (1999) 307–334
0033–4553/99/040307–28 $ 1.50 + 0.20/0

Pure and Applied Geophysics

Seismic Cycles and the Evolution of Stress Correlation in Cellular Automaton Models of Finite Fault Networks

CHARLES G. SAMMIS[1] and STEWART W. SMITH[2]

Abstract—A cellular automaton is used to study the relation between the structure of a regional fault network and the temporal and spatial patterns of regional seismicity. Automata in which the cell sizes form discrete fractal hierarchies are compared with those having a uniform cell size. Conservative models in which all the stress is transferred at each step of a cascade are compared with nonconservative ("lossy") models in which a specified fraction of the stress energy is lost from each step. Particular attention is given to the behavior of the system as it is driven toward the critical state by uniform external loading. All automata exhibit a scaling region at times close to the critical state in which the events become larger and energy release increases as a power-law of the time to the critical state. For the hierarchical fractal automata, this power-law behavior is often modulated by fluctuations that are periodic in the logarithm of the time to criticality. These fluctuations are enhanced in the nonconservative models, but are not robust. The degree to which they develop appears to depend on the particular distribution of stresses in the larger cells which varies from cycle to cycle. Once the critical state is reached, seismicity in the uniform conservative automaton remains random in time, space, and magnitude. Large events do not significantly perturb the stress distribution in the system. However, large events in the nonconservative uniform automaton and in the fractal systems produce large stress perturbations that move the system out of the critical state. The result is a seismic cycle in which a large event is followed by a shadow period of quiescence and then a new approach back toward the critical state. This seismic cycle does not depend on the fractal structure, but is a direct consequence of large-scale heterogeneity of these systems in which the size of the largest cell (or the size of the largest nonconservative event) is a significant fraction of the size of the network. In essence, seismic cycles in these models are boundary effects. The largest events tend to cluster in time and the rate of small events remains relatively constant throughout a cycle in agreement with observed seismicity.

Key words: Regional seismicity, seismic cycle, cellular automation, critical point, fractals.

Introduction

Regional seismicity has many characteristics of a critical system including a power-law Gutenberg–Richter magnitude frequency relation and a fractal spatial

[1] Department of Earth Sciences, University of Southern California, Los Angeles, CA 90089-0740, U.S.A.
[2] Geophysics Program, University of Washington, Seattle, WA, U.S.A.

distribution of hypocenters (HIRATA, 1989a,b; ROBERTSON *et al.*, 1995). This had led many investigators to explore the possibility of using formalisms from statistical physics to model the spatial, temporal and magnitude distributions (ALLÈGRE *et al.*, 1982; ALLÈGRE and LE MOUEL, 1994; RUNDLE, 1988a,b, 1989, 1993; RUNDLE *et al.*, 1995, 1996; SMALLEY *et al.*, 1985; SAHIMI *et al.*, 1993a,b; SORNETTE and SORNETTE, 1990; NEWMAN *et al.*, 1994; SORNETTE and SAMMIS, 1995; SALEUR *et al.*, 1996a,b; MOREIN *et al.*, 1997; FISHER *et al.*, 1997; DAHMEN *et al.*, 1998). In the course of analyzing seismicity as a critical phenomenon, an interesting controversy has arisen as to the interpretation of such models and their implications. The central issue is whether the crust is in a continuous state of self-organized criticality (SOC), or whether it repeatedly approaches and retreats from a critical state. The working hypothesis for this later view is that a large regional earthquake is the end result of a process in which the stress field becomes correlated over increasingly long scale-lengths. The largest event cannot occur until regional criticality has been achieved. This large event then destroys criticality on its network creating a period of relative quiescence after which the process repeats by rebuilding correlation lengths toward criticality and the next large event.

The reason this question of continuous vs. discontinuous criticality is important is that it bears directly on the question of whether earthquakes can be forecast. BAK and TANG (1989) argue that the crust is always in a state of SOC. Their analog is a uniform cellular automaton in which a ball dropped in a randomly chosen cell is equally likely to start an avalanche of any size at any time. The crustal equivalent is that all small earthquakes have the same probability of growing into a great event. This model has been used by GELLER *et al.* (1997) as a physical basis for their recent assertion that earthquake prediction is inherently impossible. If the earth is always in a state of SOC, they may be correct. However, if a large shock moves some associated region away from criticality, then the seismicity associated with the subsequent return to criticality (and the next large event) is expected to have a number of observable characteristics including an increase in event size with growing stress correlation length, and an energy release rate which increases as a power law of the time-to-failure.

The central question thus becomes: is the crust in a continuous state of SOC? Several recent observations suggest not. SYKES and JAUMÉ (1990) and TRIEP and SYKES (1997) have found that large earthquakes are preceded by a cluster of intermediate-sized events (within $2M_w$ units of the main shock) in a large surrounding region. KNOPOFF *et al.* (1996) found that all 11 earthquakes in California since 1941 with magnitudes greater than 6.8 were preceded by an increase in the rate of occurrence of earthquakes with magnitudes greater than 5.1 in the appropriate tectonic domain. There is also mounting evidence that the rate of intermediate-sized events decreases following a large earthquake—an observation generally interpreted as resulting from a regional stress shadow. Such shadows have been documented by SYKES and JAUMÉ (1990) following the 1989 Loma Prieta earth-

quake, by TRIEP and SYKES (1997) following the 1950 Assam shock, by HARRIS and SIMPSON (1996) following the 1857 Fort Tejon earthquake, and by Jones following the 1952 Kern County and 1992 Landers earthquakes. BOWMAN and SAMMIS (1997) and TRIEP and SYKES (1997) have suggested that these shadows represent the retreat of a region from a state of SOC. SORNETTE and SAMMIS (1995), SAMMIS *et al.* (1996), and SALEUR *et al.* (1996a,b) also argue that the observed power-law buildup of intermediate events before a great earthquake represents the approach of the appropriate region toward a state of SOC.

The power-law increase in regional seismicity before large events was first documented by BUFE and VARNES (1993) and BUFE *et al.* (1994) who found that the clustering of intermediate events before a large shock produces an increase in cumulative regional energy release (or in cumulative regional Benioff strain, $\varepsilon(t) = \sum_{j=1}^{N(t)} E_j^{1/2}$) that can be fit by a power-law time-to-failure relation of the form

$$\varepsilon(t) = A + B(t_c - t)^m \tag{1}$$

where t_c is the time of the large event, B is negative and m is usually about 0.3. SORNETTE and SAMMIS (1995) showed that the power law (1) is expected if the largest event is viewed as some sort of critical point for the region. In this case the mathematical techniques developed in statistical physics to describe critical phase transitions can be applied to seismicity. One technique, the renormalization group (RG), leads directly to (1) (see SALEUR *et al.*, 1996a,b for a discussion of the application of the RG to regional seismicity). The renormalization group also explains the observed clustering of large events prior to the largest shock (SYKES and JAUMÉ, 1990) in terms of the growth of the spatial correlation length of the regional stress field. In this view, larger events are not possible until the stress field is correlated at a sufficient length to produce them. Before this time small events are unable to jump barriers and grow into big events. Only when criticality is reached is the stress field correlation on all scale lengths permitting events of all sizes up to the largest possible on the given fault network. The implication is that the smaller events are the agents by which longer stress correlation lengths are established—they effectively smooth the stress field at larger scale lengths (SAMMIS *et al.*, 1995; BEN-ZION, 1996). It is important to note that the largest regional event need not occur at t_c in Equation (1). Rather, this is the time when the region reaches the critical state and a large event is possible.

An important observational question arises when fitting Equation (1) to seismicity data: how is the size of the "critical region" to be chosen for a given event? BOWMAN *et al.* (1999) showed that, for all 12 California earthquakes having magnitude $m > 6.2$, a critical region size could be found which optimized the fit to Equation (1). Moreover, they found that the logarithm of the radius R of these optimal critical regions scaled as the magnitude

$$\log R \propto 0.5\, m \tag{2}$$

and that they could reject the null hypothesis that their fits were consistent with a random catalog with 99.9% confidence. A similar study by BREHM and BRAIL (1998) analyzed nineteen events from the New Madrid Seismic Zone and found $\log R \propto 0.75$ m. JAUMÉ and SYKES (1999) combined the two data sets and found the best fit is $\log R \propto 0.36$ m in better agreement with Equation (2). It is interesting that Equation (2) is compatible with the scaling of preparatory region with magnitude found by KEYLIS-BOROK and MALINOVSKAYA (1964) using a different method.

Another testable hypothesis that has emerged from the critical point model for seismicity is the possibility of log-periodic fluctuations in seismicity approaching criticality. SORNETTE and SAMMIS (1995) showed that if the spatial renormalization can only be made at a discrete fractal hierarchy of scale lengths, then the critical exponent is imaginary in time and Equation (1) becomes (to a first approximation, retaining only leading term in the periodicity)

$$\varepsilon(t) = A + B(t_c - t)^m \left[1 + C \cos\left(2\pi \frac{\log(t_c - t)}{\log \lambda} + \psi \right) \right]. \tag{3}$$

Such log-periodicity has been documented in several cases (SORNETTE and SAMMIS, 1995; VARNES and BUFE, 1996), but it has yet to be established as a universal precursor to large events. The modeling study presented below suggests that it may not be universal. However, if observed, log-periodicity allows a more precise estimate of t_c (SORNETTE and SAMMIS, 1995; SAMMIS *et al.*, 1996).

The physical cause of log-periodicity is still an open question. One possibility is the existence of a discrete fractal hierarchy in the regional fault network. Such structures may be simulated by a discrete hierarchical fractal automaton (BARRIER and TURCOTTE, 1994; HUANG *et al.*, 1998) which is explored further in this paper. Another possibility is that the earthquake sequence develops its own discrete hierarchy through stress shielding interactions in a highly heterogeneous region. This possibility has been demonstrated experimentally by ANIFRANI *et al.* (1995), numerically by SAHIMI and ARBABI (1996), and analyzed by HUANG *et al.* (1997). A third possibility is that log-periodicity may arise from random fluctuations in the power-law approach to criticality (HUANG, personal communication). Although not physically interesting, the observation of randomly generated log-periodic oscillations can be taken as evidence of power-law behavior and used to help determine t_c.

In this paper, we use cellular automaton models to explore conditions under which these simple systems alternately build then destroy stress correlation thereby simulating regional seismic cycles. We begin with the homogeneous conservative automaton originally formulated by BAK *et al.* (1987) and explore the power-law scaling and growth of stress correlation as the initial loading transient moves the system toward SOC. Once SOC is established in this system, large events do not destroy stress correlation and the system remains critical. Large events in the SOC

state do not show the precursory increases in seismicity or post-event quiescence observed in real catalogs. We next explore the uniform nonconservative automaton discussed by OLAMI *et al.* (1992) in which a fraction of the energy is lost from each subevent in a cascade. We find that the largest cascades in this model destroy stress correlation thus moving the system out of the critical state and producing seismic cycles having many characteristics observed in real catalogs. Finally, we explore the discrete hierarchical fractal automaton previously studied by BARRIER and TURCOTTE (1994) and HUANG *et al.* (1998). The largest events in this model also destroy stress correlation and produce seismic cycles for cases where the scale of the structural heterogeneity associated with the fractal structure is comparable to the scale of the network. We expand the previous work of HUANG *et al.* (1998) by exploring a range of fractal dimensions, by exploring the relationship between the scale of the heterogeneity and the size of the network, and by separating the effects of energy loss from effects of the discrete hierarchical structure. Our general result is that seismic cycles in the automaton model result from the finite size of the network and either heterogeneity on a scale comparable to the size of the network, a significant loss of energy from the network during the event, or a combination of both.

A Cellular Automaton Model for Regional Seismicity

We begin with a review of the basic elements of the cellular automaton, first exploring the homogeneous automaton developed by BAK *et al.* (1987) for conservative systems and extended by OLAMI *et al.* (1992) for nonconservative systems which map onto the BURRIDGE-KNOPOFF (1967) spring-block model of earthquakes. We then review the conservative fractal automaton as defined by BARRIER and TURCOTTE (1994) and extended to nonconservative cascades by HUANG *et al.* (1998).

The Homogeneous Cellular Automaton with no Losses

Since the homogeneous conservative automaton is known to exhibit SOC (BAK and TANG, 1989) we use it here to establish the conditions which characterize SOC as a basis for comparison with the nonconservative and fractal systems. The uniform cellular automaton defined by BAK *et al.* (1987) consist of a 2-D array of equal sized cells as in Figure 1a. The array is loaded by dropping "balls," one at a time, into randomly selected cells. A cell is considered full when it contains three balls. If a fourth ball is added to a full cell, the contents of that cell are distributed equally to the four nearest neighboring cells. If this redistribution results in four balls in a neighboring cell, then that cell also unloads to its four neighbors (one of which goes back into the original cell), and so on. Cells that are on the edge of the

array dump one ball off the array while corner cells dump two balls off the array. When no cell contains four balls, the cascade ends and the random dropping of balls onto the array resumes. The term "conservative" is used here to denote the conservation of balls during each subevent in a cascade, even though balls are lost from the edges of the network.

The size of a cascade is measured by the number of cells that are involved. Cascades of all sizes occur from one cell up to the size of the array. Once the number of balls on the array reaches equilibrium, the distribution of avalanche sizes follows a power law and the system is in a state of self-organized criticality (SOC).

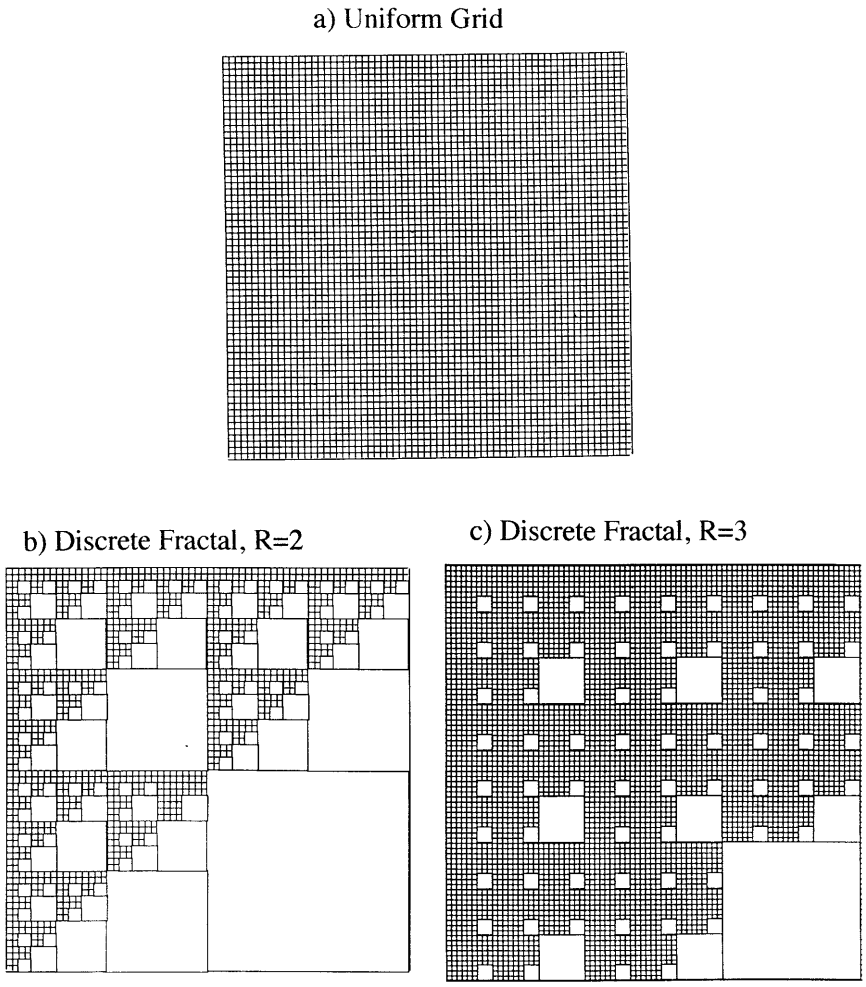

Figure 1
Grids used for (a) the uniform homogeneous automaton, (b) the discrete hierarchical fractal automaton with rescale factor $R = 2$, and (c) the discrete hierarchical fractal automaton with rescale factor $R = 3$.

A characteristic of SOC is that the individual events are not predictable in time, or space, or magnitude. The fact that regional seismicity follows the Gutenberg–Richter power-law relation between number and magnitude suggests the possibility that the crust is in a state of SOC, and that regional seismicity is a member of the class of phenomena described by the homogeneous automaton. If this is true, then the time place and magnitude of individual earthquakes is inherently unpredictable.

Interpreting regional seismicity in terms of the cellular automaton, the balls can be viewed as representing increments of stress, strain, or stored elastic energy—all are equivalent measures in an elastic solid. We will discuss the process in terms of stored energy. Each ball drop represents an equal increment of time. The random loading of the array corresponds to a slowly increasing tectonic stress while the unloading of a cell represents the stress redistribution associated with an earthquake. A larger cascade represents a spatially larger redistribution of stress and therefore corresponds to a larger earthquake. The cascades are assumed to take no time since the time-scale associated with an earthquake is short in comparison to the time-scale associated with the tectonic loading. Although the long-term average loading rate is constant for the array and may be viewed as due to the constant motion of tectonic plates, the random dropping of balls continuously introduces random fluctuations at the smallest scale. In the geological context, this corresponds to a continuous, small-scale, spatially random roughening of the stress field. A physical source for such small-scale roughening is not obvious. One might assert that it is the result of small earthquakes that produce stress redistribution at scale-lengths less than or equal to that of the smallest box. However, as will be discussed below, small events are expected to smooth the field at scale-lengths larger than themselves, not roughen it. The amplitude of this small-scale roughening in the model can be decreased by increasing the failure threshold from four balls to, say, 400 balls in which case 100 balls are distributed to each of the four neighbors. The roughening produced by each random ball drop is thereby proportionally reduced. We have found that such reduction in the amplitude of small-scale roughening has no observable effect on the temporal or spatial behavior of the automaton.

It is also possible to formulate the automaton such that the loading is equally distributed to all cells (OLAMI *et al.*, 1992). In this case the energy in each cell is not an integral number of balls, but a real number between 0 and some arbitrary threshold which we take to be 1. The cell with the maximum energy $s_{\max}$ is identified and the energy in each cell is increased by $1 - s_{\max}$. The energy in the maximal cell is then set to zero and its energy of 1 is distributed equally among each of its four nearest neighbors that receive 0.25 each. If this redistribution results in another cell having an energy $s \geq 1$, the energy in that cell is set to 0 and its energy, which may be greater than 1, is distributed in equal portions to its four nearest neighbors (which includes reloading the cell which failed initially). The cascade continues until no cell has $s \geq 1$. The time-scale in this case is set by the assumption of a uniform loading rate which requires that time increments be

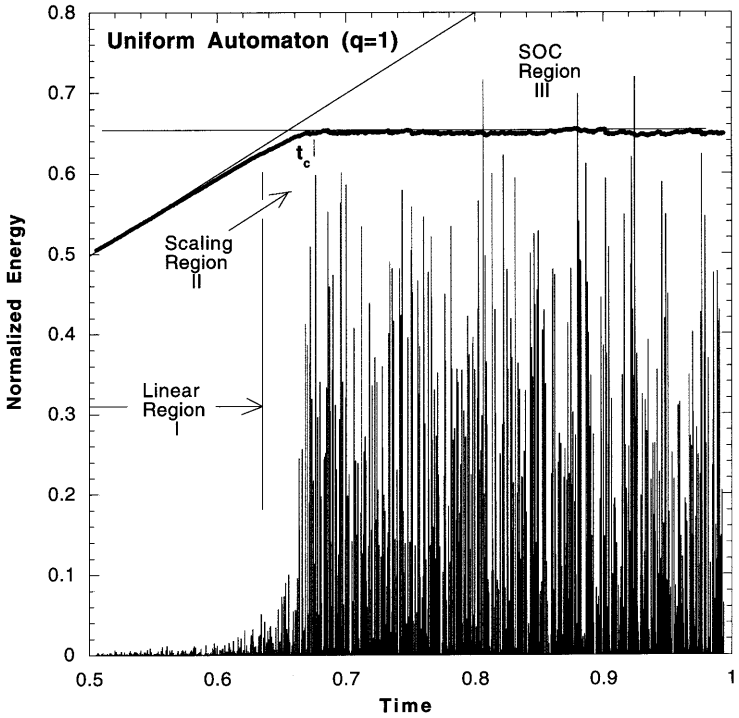

Figure 2
Normalized energy vs. normalized time for the uniform homogeneous automaton with no losses ($q = 1$). The upper heavy line shows energy on the grid while the catalog of events is shown below. The linear, scaling, and SOC regions are identified as discussed in the text.

directly proportional to increments in the energy. Since the constant of proportionality is arbitrary, we choose it to be unity, i.e., we take $\Delta t = \Delta s$. This means that a cell having an energy of 0.6 will fail in 0.4 time units if no other energy is added from neighboring cells. Again we assume that cascades take no time. In this case the automaton is initiated by assigning a random number in the interval (0,1) to each cell. This random initial distribution can be interpreted as the result of a combination of elastic heterogeneity and the prior history of events. This system evolves to an equilibrium state that is independent of the random starting distribution. We use uniform loading for all the simulations presented in this paper and discuss those results which are affected by this choice.

Figure 2 shows the catalog generated by a homogeneous 64×64 automaton with uniform loading and no losses. As in BAK and TANG (1989) the total number of cells which spill during a cascade is taken as the size of the event and as a measure of the energy released by the event. Also shown on this figure is the average energy density in the system. Initially, the average energy density increases linearly from its starting value of 0.5 (since each cell is given a random initial energy

between 0 and 1). The initial slope is one since most of the energy added to the grid through the loading process remains on the grid. As the energy density grows, the size of the largest avalanche increases. As these larger avalanches begin to intersect the edges of the grid on a more regular basis, more energy is lost from the grid per unit time and the slope of energy-density vs. time curve in Figure 2 decreases. Eventually, the energy density on the grid becomes constant—energy is lost from the edges at the same rate it is added through the loading process.

We can thus identify three regions in the energy density curve labeled I, II, and III in Figure 2. Region I is the initial transient where most of the energy added to the grid remains on the grid. Region II is the transition region between region I and the steady-state region III that we identify as characterizing the SOC state. By fitting straight lines to regions I and III in Figure 2, the transition region II can be seen to extend from about $t = 0.64$ to $t = 0.67$. We will show below that region II is the "scaling region" close to SOC where the energy released by the cascades can be fit to the power law in Equation (1). Note that t_c does not correspond to the largest event in the sequence. Figure 3 shows the cumulative energy released by the events in Figure 2. The average energy density and three regions from Figure 2 are also plotted for reference.

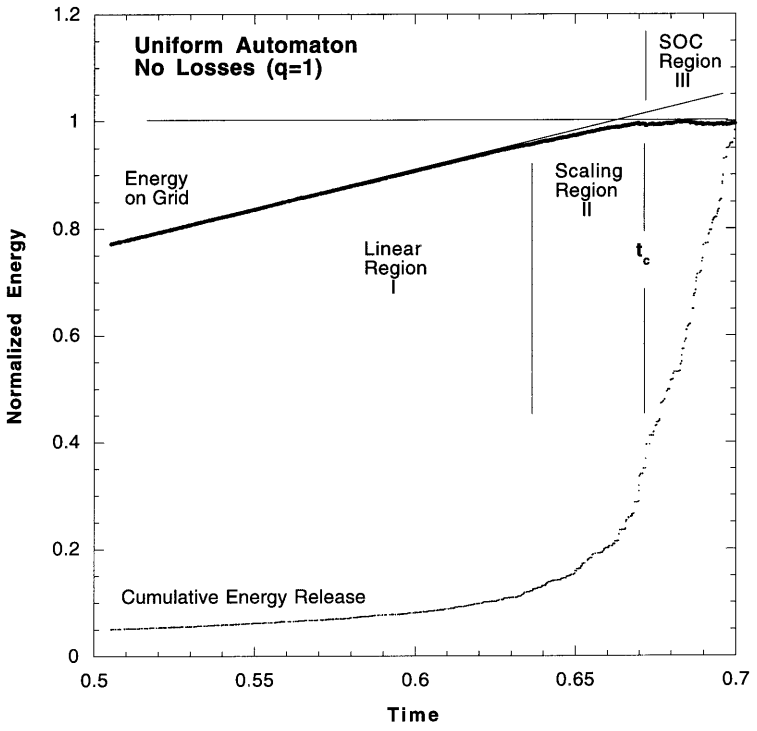

Figure 3

Cumulative release of scaled energy as a function of time for the uniform homogeneous automaton with no losses. The energy on the grid and regions I–III are replotted from Figure 2 for reference.

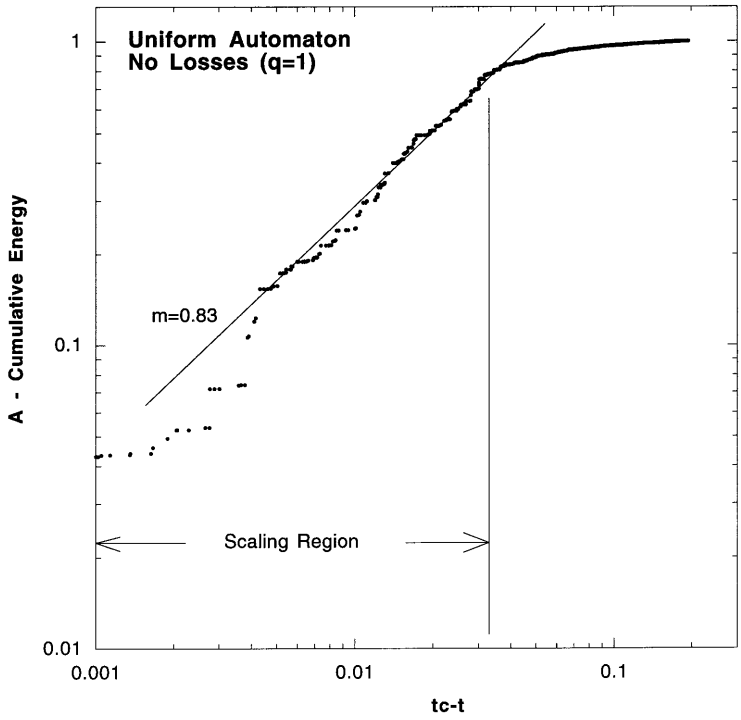

Figure 4
For the cumulative energy in Figure 3, the quantity $\log(A - \text{cumulative energy})$ is plotted as a function of the logarithm of the distance from the critical point, $\log(t_c - t)$, in order to test the fit to Equation (1). The fit is linear in the scaling region II as expected.

To further investigate region II we fit Equation (1), the expected behavior in the scaling region close to criticality (SORNETTE and SAMMIS, 1995). Both t_c and A in this equation are known since A is the value of the cumulative energy when $t = t_c$ (see Fig. 3). Figure 4 is a plot of $\log(A - \Sigma E)$ vs. $\log(t_c - t)$. The linear portion of this curve indicates the scaling region II in which Equation (1) applies (with $m = 0.83$). Note that this region extends to about $t_c - t = 0.03$. Since we took $t_c = 0.67$ the scaling region covers $0.64 < t < 0.67$, in agreement with the transition region II identified in Figure 2.

The rate of occurrence of earthquake over a broad region is well described by the GUTENBERG–RICHTER (1956) frequency-magnitude relation

$$\log_{10} N(M > \mathrm{m}) = a - b\mathrm{m} \tag{4}$$

where N is the number of events with magnitude M greater than m. Using the energy magnitude relation

$$\log_{10} E = c + d\mathrm{m} \tag{5}$$

The Gutenberg–Richter relation becomes a power-law relation for the number of earthquakes having E_0 greater than E

$$N(E_0 > E) \sim E^{-b/d} = E^{-B} \tag{6}$$

with B commonly in the range 0.80–1.05. The observation that the cellular automaton produces this distribution of event sizes is commonly cited as evidence that the crust is in a state of SOC (BAK and TANG, 1989; OLAMI *et al.*, 1992). We also find that events in the SOC region ($t > t_c = 0.67$) are consistent with Equation (6).

We end our discussion of the conservative homogeneous automaton by exploring the growth of stress correlation during the approach to criticality and the fluctuations in correlation in the SOC state. By stress correlation we mean the size of "critical clusters" which would cascade if one element were triggered. The simplest measure of stress correlation is the size distribution of the avalanches themselves. Since we are most interested in the largest critical cluster at any time, we can simply identify the largest event as a function of time. The only problem with this approach is that, at any given time, the largest cluster may not be triggered. We therefore plot the largest event in successive time intervals of $\Delta t = 0.01$ to minimize nucleation effects. Figure 5a shows the maximum event as a function of time for the case shown in Figures 2–4. The correlation length grows steadily in region I, at an accelerated rate in the scaling region II, and then remains relatively constant in the SOC region III. Figure 5b shows the rate of small events (events which have an area $< 5\%$ of the maximum event area observed over the entire time shown). Note that rate of small events remains relatively constant over the entire time interval in agreement with observations by ELLSWORTH *et al.* (1981).

The Homogeneous Cellular Automaton with Losses

OLAMI *et al.* (1992) explored the effect of a loss factor $0 < q < 1$ on the behavior of the uniformly loaded homogeneous automaton. In this case, if a cell contains an energy $s \geq 1$, its energy is set to zero and the energy qs is distributed equally to its four neighbors. The justification for this loss factor is clear if the automaton is being used to simulate the complexity of slip on a fault-plane. In this case q represents the fraction of energy lost to friction, to the formation of fault gouge, and to seismic radiation. However, the justification of q is not as clear when the automaton is being used to simulate regional seismicity. In this case, a cascade does not represent a growing slip patch, but the transfer of shear stress released by an earthquake. In an abstract sense, if s is viewed as the elastic energy stored in a cell, then the overall loss of energy from the system could be viewed as representing the losses to friction and other forms of nonelastic deformation, fragmentation, and radiation. Since this loss limits the size of the cascade, it could be argued that an earthquake with larger nonelastic losses transfers stress to a smaller region.

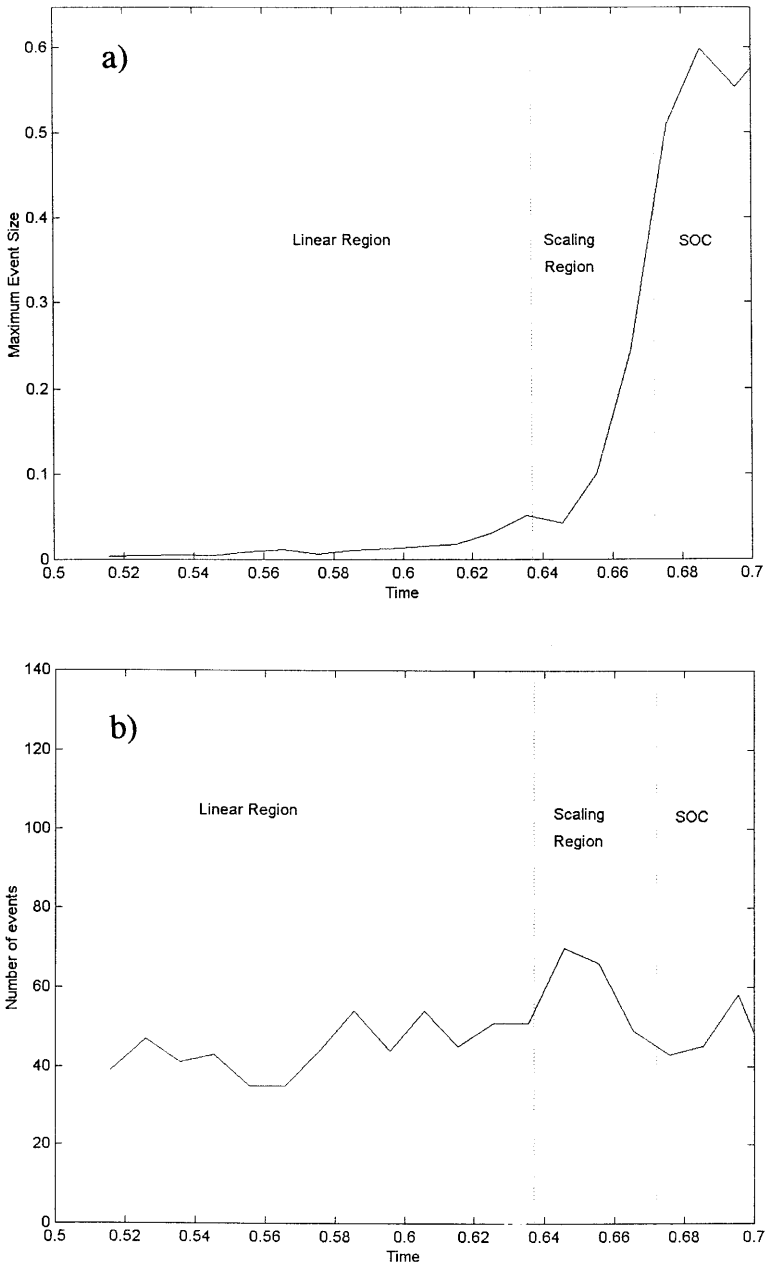

Figure 5
Temporal distribution of event sizes in the uniform automaton without losses. In panel (a) the maximum event size is plotted as function of scaled time illustrating the growth of correlation length in the scaling region leading up to the critical point and the relative constancy of correlation in the SOC region. Panel (b) shows the temporal distribution of small events which remains approximately constant in agreement with observed seismicity.

The q factor will be shown below to introduce memory into the automaton. The largest events leave "stress shadows" that move the system out of the critical state. This result seems to be at odds with OLAMI *et al.* (1992) who claim that their nonconservative automaton displays SOC based on its generation of power-law scaling of event sizes. However, KLEIN and RUNDLE (1993) point out that the scaling with system size found by OLAMI *et al.* is not consistent with their model being at the true scaling limit and their conclusions about critical behavior are therefore suspect. GRASSBERGER (1994) developed a fast computational algorithm that allowed him to explore the nonconservative model on larger grids and for longer times. He found that the scaling observed by OLAMI *et al.* was largely a boundary effect that is observed only in relatively small systems or in larger systems during the long transient period. Grassberger suggested that such boundary effects, or other forms of frozen heterogeneity, might be important in the earthquake problem and we agree. The significant factor appears to be the size of the largest event relative to the size of the network. Where the size of the largest event in the conservative automaton is limited only by the size of the system, we will show below that the size of the largest event in the nonconservative system is limited by the losses during the cascade. Significant retreats from the critical state only occur when the size of the largest event is a significant fraction of the size of the network.

Figure 6 shows the catalog generated by this model for $q = 0.9$ and the average energy density in the grid for selected values in the range of $0.5 \leq q \leq 1.0$. There are several striking differences between this figure and Figure 2. Most notably, the events here are much smaller. We found that the size of the events is proportional to $1/(\ln q)$. For $q < 1$, the size of the events is limited by the losses, not by the size of the grid. In fact, the size of the events is controlled by the clustering statistics of the array of random initial values assigned to the cells. A simple statistical analysis of an $n \times n$ array of random initial values in the range (0,1) predicts that the maximum event size should vary approximately as $(\ln 4 - 2 \ln n)/\ln q$ which we have verified with simulations over a range of n and q.

Another contrast with Figure 2 is that the average energy on the grid in Figure 6 shows periodic structures in what should be the SOC region III. The period of this behavior, T, increases with decreasing q as $T = 1 - q$. This periodicity is also evident in the catalogs and appears to be due to stress shadows left behind by the large events. To understand why $T = 1 - q$, consider a cell that nucleates a large cascade. Initially, its load drops from 1 to 0. For a large cascade, it is likely that this will cause its four nearest neighbors to fire each of which returns $q/4$ units of stress to the initial cell. Hence, the nucleating cell ends up with a load of q and will therefore trigger another large cascade after $T = 1 - q$ time units have passed. Note that the relation $T = 1 - q$ holds at the extremes of $q = 1$ and $q = 0$. The case $q = 1$ corresponds to full stress transfer and SOC where there is no periodicity ($T = 0$). The case $q = 0$ corresponds to no stress transfer in which case the initial random distribution of loads is preserved and leads to an exact repetition of the catalog

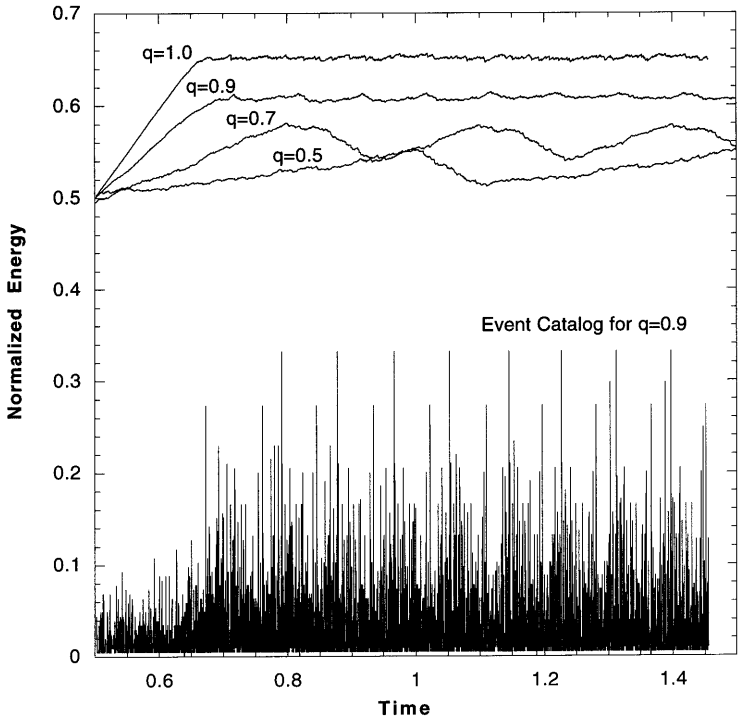

Figure 6
Normalized energy vs. normalized time for the uniform homogeneous automaton with losses ($q < 1$). The upper heavy lines shows energy on the grid for a range of q while the catalog of events for $q = 0.9$ is shown below. Note the periodic fluctuations in energy on the grid and related periodicity in the catalog.

after each full loading period $T = 1$ (recall that we defined the threshold of 1 to correspond to one time unit). It is interesting that this periodicity does not appear for the case of strong random loading (a four ball-threshold). In this case the memory of stress shadows is destroyed by the random fluctuations introduced through loading.

Figure 7 shows the cumulative energy corresponding to the catalog in Figure 6. Note that the three regions can also be identified in the initial transient, but the interpretation of region III as SOC is questionable because of the predictability introduced by the periodic structure. The parameters A and t_c identified in Figure 7 are used in Figure 8 to test the suitability of Equation (1) to describe the scaling region II. Note that an apparent scaling region can be identified extending to $t_c - t = 0.05$ with a slope of $m = 0.8$. Figure 9a shows the largest event (our proxy for maximum correlation length) as a function of time. Note that the losses produce fluctuations in the maximum correlation length in region III which correspond to the periodic structures in the energy on the grid and in the catalog (Fig. 6). Figure

9b shows that the rate of small events also remains relatively constant during the initial approach of lossy systems toward criticality. In Figure 7 we have only analyzed the initial transient for direct comparison with the conservative case. We have also analyzed the increasing portions of the cycles and found that they also can be fitted to Equation (1), although there is a bit more scatter.

We therefore interpret the periodic fluctuations in Figure 6 as reflecting the repeated approach and retreat of the system from the critical state. It is interesting that the retreat from criticality is not caused by a single large event. Rather, the decrease of energy on the grid is caused by a swarm of large events across the grid over the entire decreasing interval. Often the largest event occurs at the end of the swarm and marks the onset of the increase in grid energy leading to the next swarm. Note that as q decreases, the average energy on the grid in region III decreases while the amplitude of the fluctuation increases. Both effects are related to the decrease in the maximum size of the events with decreasing q. In general, as energy on the grid increases the correlation length increases. However, when the correlation length reaches the size of the maximum event for the given q, the events

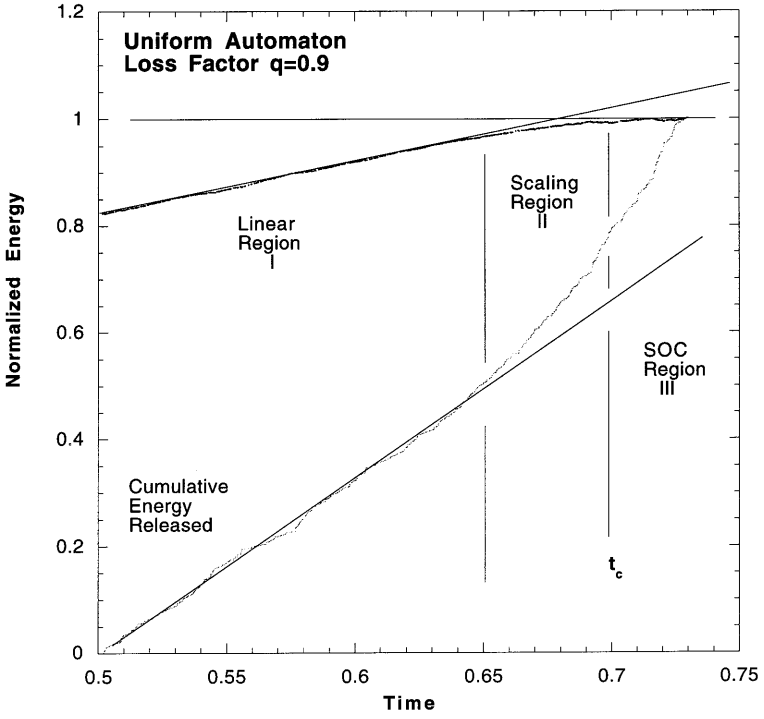

Figure 7
Normalized energy on the grid and cumulative energy released as a function of scaled time for the uniform automaton with loss factor $q = 0.9$. Note that regions I, II, and III can also be identified in this case.

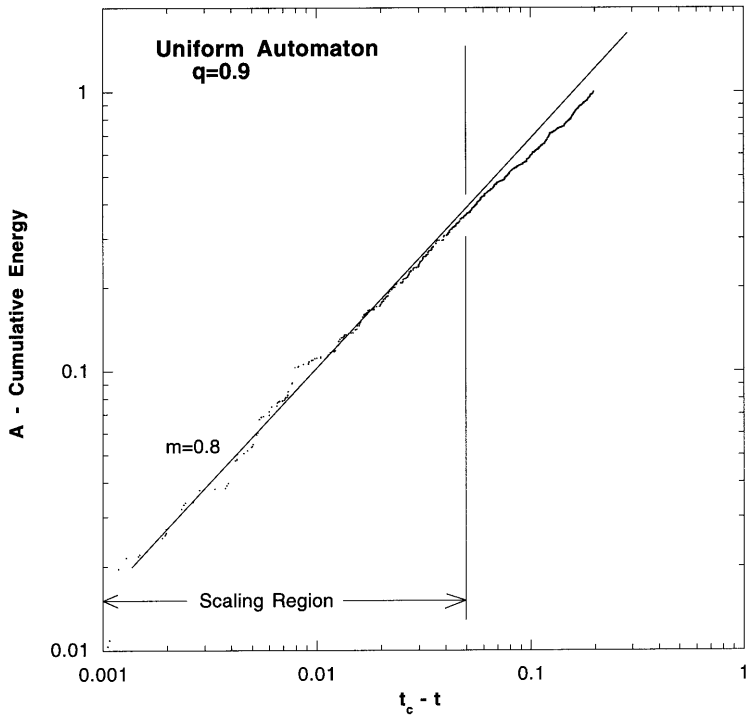

Figure 8
For the cumulative energy in Figure 7, the quantity $\log(A - \text{cumulative energy})$ is plotted as a function of the logarithm of the distance from the critical point, $\log(t_c - t)$, in order to test the fit to Equation (1). The fit is linear in the scaling region II for the loss factor $q = 0.9$.

of that size unload the grid ending the cycle. Since this correlation length is reached at a lower grid load for a lower q the average energy on the grid decreases with decreasing q. Also, for a given grid size n, there are statistically more limiting events at lower q since they are smaller. Since the energy ΔE lost by a limiting event is almost independent of q, there is more unloading and hence larger fluctuations at smaller q. To see why ΔE is almost independent of q, write the energy lost per event as the energy lost per cell, $(1 - q)$, times the size of the event and approximate $\ln q \approx (1 - q)$ for $q \approx 1$

$$\Delta E \approx (1 - q)\frac{\ln 4 - 2 \ln n}{\ln q} \approx (1 - q)\frac{2 \ln n - \ln 4}{(1 - q)} = 2 \ln n - \ln 4. \tag{7}$$

Hence, for $q < 1$ the system never reaches the critical state but is moved away by events at the largest allowable size.

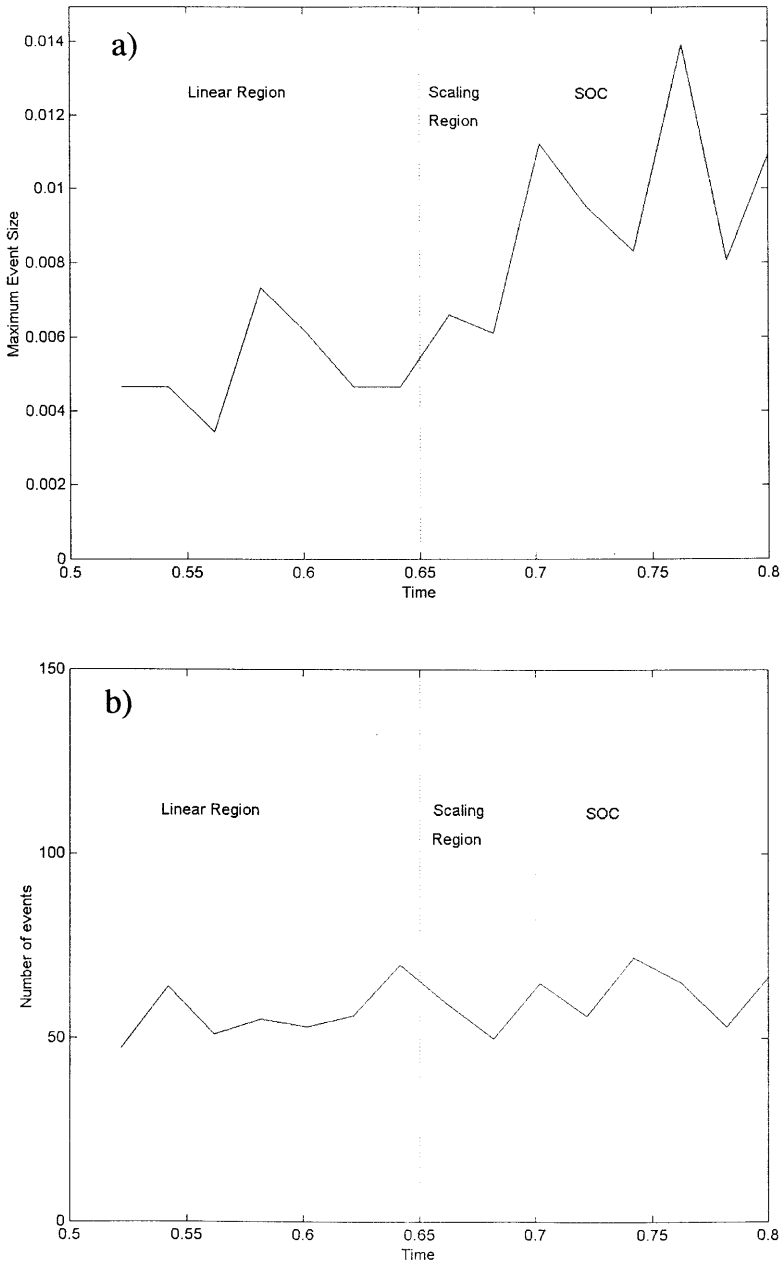

Figure 9

Temporal distribution of event sizes in the uniform automaton with loss factor $q = 0.9$. In panel (a) the maximum event size is plotted as function of scaled time. The correlation length again grows in the scaling region leading up to the critical point but the maximum event size fluctuates for $t > t_c$ in concert with the fluctuations in energy on the grid in Figure 6. Panel (b) shows the temporal distribution of small events which remains approximately constant in agreement with observed seismicity.

The Conservative Fractal Automaton

BARRIER and TURCOTTE (1994) explored the fractal automaton shown in Figure 1b. This fractal is discrete in that it is only strictly self-similar when rescaled by a factor of $R = 2$. For the case of uniform loading, the smallest cells still unload when they reach a threshold of 1, but progressively larger cells do not unload until they reach a larger load equal to their area.

Barrier and Turcotte also gave a slightly different interpretation to the meaning of a cascade. Unlike the uniform automaton where each cascade represents one earthquake, they view the failure of each cell as representing an earthquake. This is equivalent to viewing each cell as an individual fault and assuming a characteristic earthquake model in which the size of the earthquake is proportional to the size of the cell. For each cascade, they identify the largest cell to spill as the mainshock. Those members of the cascade that spill before the mainshock are identified as foreshocks while those that spill afterwards as aftershocks. Their principal result is that while all large events have many aftershocks, only about 28% have foreshocks—a result that mimics actual seismic statistics.

In the modeling given here, as in HUANG *et al.* (1998), the entire cascade is viewed as one event. The assumption is that the time-scale of foreshocks and aftershocks is short in comparison to the time-scale associated with tectonic loading. The stress redistribution associated with the foreshocks and aftershocks is combined with that caused by the mainshock. These models capture two aspects of real seismicity missing from the homogeneous automaton: large events are more likely to occur on pre-existing large structures and regional fault networks tend to have a hierarchical fractal structure (AVILES *et al.*, 1987; OKUBO and AKI, 1987; HIRATA, 1989a; ROBERTSON *et al.*, 1995; OUILLON *et al.*, 1996).

In order to investigate the effect of spatial structure on the temporal fluctuations in seismicity, we also considered the discrete fractal having a rescale factor of $R = 3$ shown in Figure 1c. For both the $R = 2$ and $R = 3$ fractals we also investigated the effects of the loss factor q discussed above. The fractal automatons were initiated by assigning a random number in the interval (0,1) to each of the 1×1 subcells of the uniform grid from which the fractal automaton is constructed. The initial load in each of the larger cells was then calculated as the average of the load in all its subcells. Therefore, the larger a cell, the more likely its initial average load was close to 0.50. The decision of when to spill a large cell was based on this average load—a cell spills when its average load reaches one.

We begin with the case of no attenuation ($q = 1$). Figure 10 shows the catalog of events and the energy on the grid during the initial transient approach to the critical state; Figure 10a is for the $R = 2$ grid in Figure 1b and Figure 10b is for the $R = 3$ grid in Figure 1c. The scaling region is again defined by the range of times where the energy on the grid has a slope of less than one and more than zero. Figure 11 shows the cumulative energy of the events for the two fractal models.

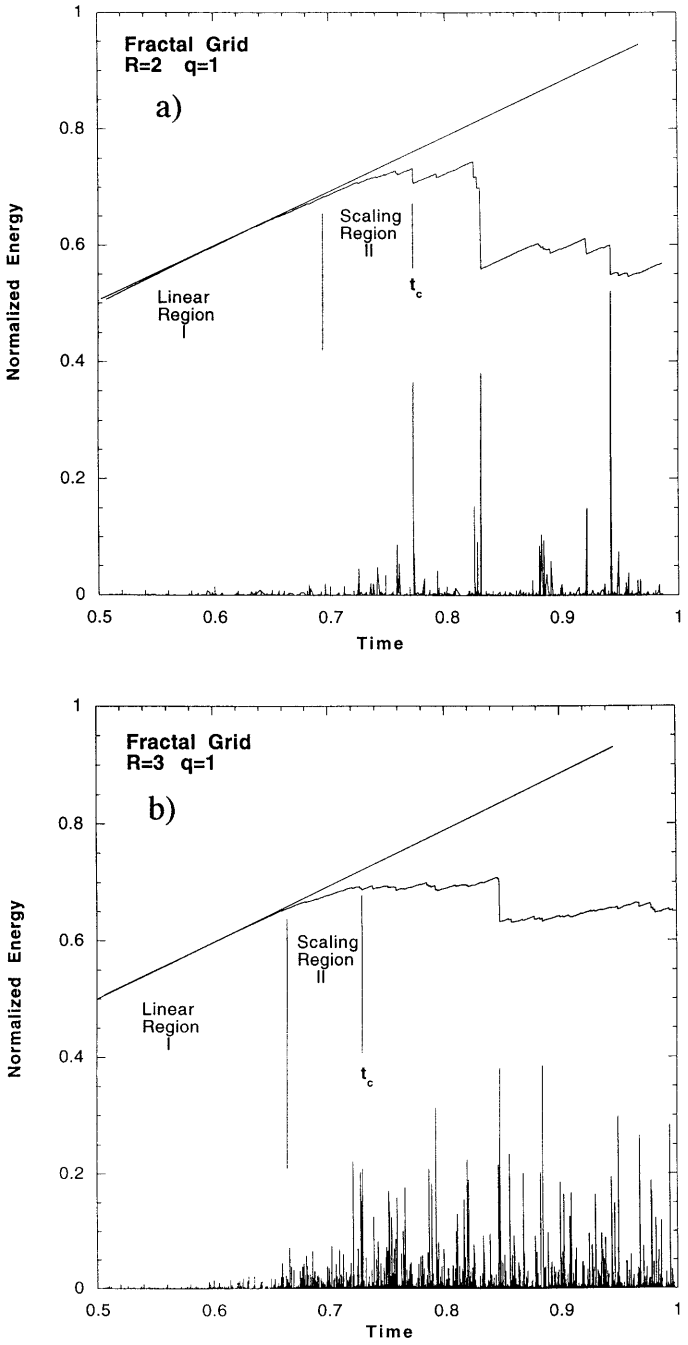

Figure 10
Total scaled energy on the grid and the catalog for the fractal grids in Figure 1 with no losses ($q = 1$). Panel (a) is for a discrete rescale factor of $R = 2$ and panel (b) for $R = 3$.

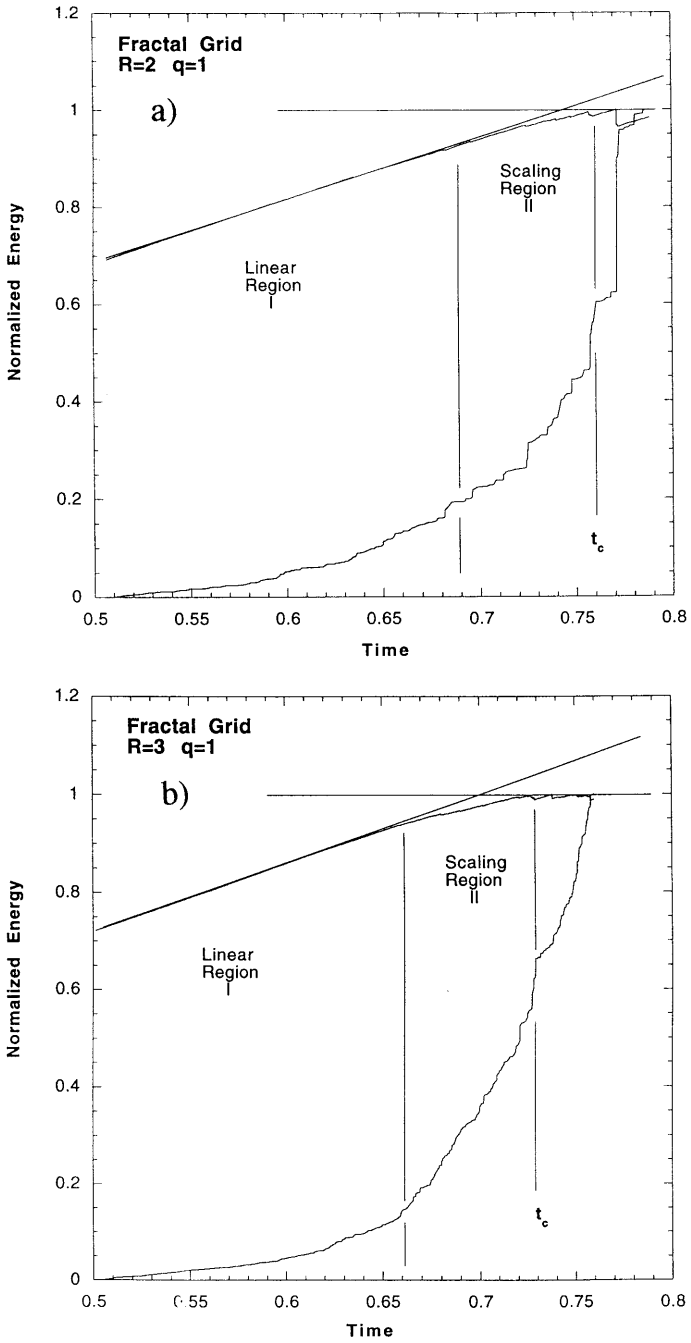

Figure 11
Cumulative scaled energy on the grid for the fractal grids in Figure 1 with no losses ($q = 1$). Panel (a) is for a discrete rescale factor of $R = 2$ and panel (b) for $R = 3$.

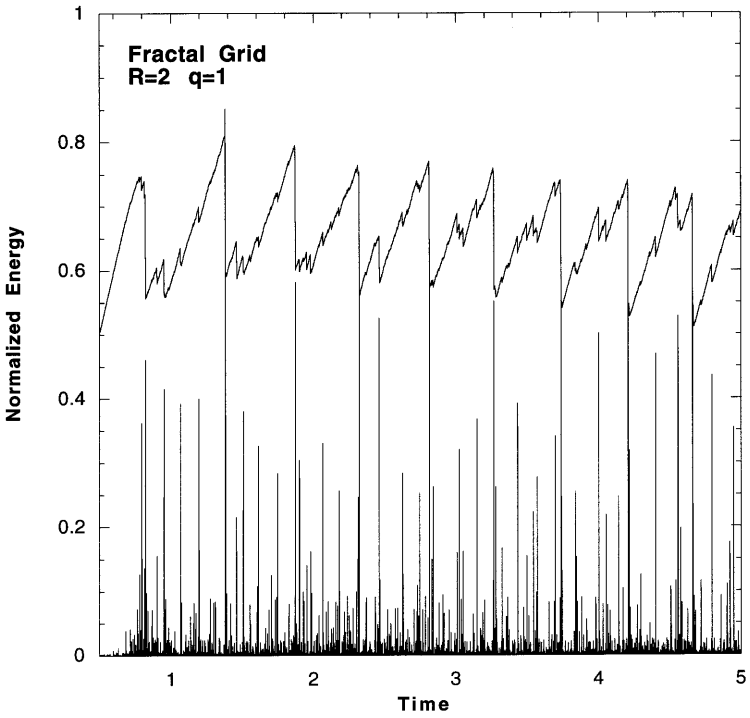

Figure 12
Energy on the grid and seismic catalog for several "cycles" of the $R = 2$ fractal automaton with no losses ($q = 1$).

Comparing these figures with the equivalent Figures 3 and 7 for the homogeneous model, note that the fractal models show larger fluctuations in the cumulative energy release. Figure 12 shows an extended catalog for the $R = 2$ grid and the energy on the grid. Note that the fractal structure introduces a periodicity into the energy on the grid. These "seismic cycles" are produced by big events in which the largest cell unloads and significant energy is lost from the grid. They do not require a fractal grid, only a grid in which the largest cell is a significant fraction of the grid size so its unloading produces an observable perturbation in the state of the system. In this view, each cycle represents the approach to criticality followed by a large event that moves the system away from the critical state. Note that the correlation and decorrelation of stress in the fractal model is forced by the structure since the larger structures are not allowed to unload until the average stress over the entire area becomes critical. When these large structures unload, the correlation of highly stressed regions is necessarily reduced.

As already demonstrated by HUANG *et al.* (1998), the discrete hierarchical structure produces log-periodic fluctuations in the power-law increase of cumulative energy release approaching the critical state of the form given by Equation (3).

Figure 13 shows the maximum event size as a function of time for the realization shown in Figure 11. The model used by HUANG *et al.* (1998) included a loss factor $q = 0.5$. We will see below that the introduction of loss into the fractal automaton enhances the amplitude of the log-periodic fluctuations.

It is important to note that while all realizations of this model produced a log-periodic sequence of discrete jumps in the maximum correlation length of the critical region as in Figure 13, this did not always produce log-periodic fluctuations in the cumulative energy release. A clear log-periodic progression of steps in cumulative energy was only observed when the intermediate events (one and two orders smaller than the maximum cell) tended to cluster in time. For those cases in which events of a given order are more evenly distributed in time, the jumps in scale only produce a subtle increase in slope of the cumulative energy producing the power-law increase before failure, but no evident log-periodic fluctuations.

The log-periodic sequence of jumps in correlation length is a direct consequence of the way in which the initial loads were assigned. Since we define the load in a box by the area average of loads in its subcells, a larger box is more likely to have an initial load close to 0.5 than is a smaller box. Since we are averaging random variables, the standard deviation of the average loads in boxes having N subcells decreases as $\sqrt{N}$. Hence, smaller boxes are more likely to trigger first because they have a larger range of loads and because there are more of them. Now, consider the $R = 2$ fractal in Figure 1b. Since there are only three second largest cells and nine third largest, it is more likely that the loads in the larger cells will cluster to produce log-periodic fluctuations in the cumulative energy. This may explain why only one or two log-periodic fluctuations are observed even though there are many more orders in the fractal hierarchy.

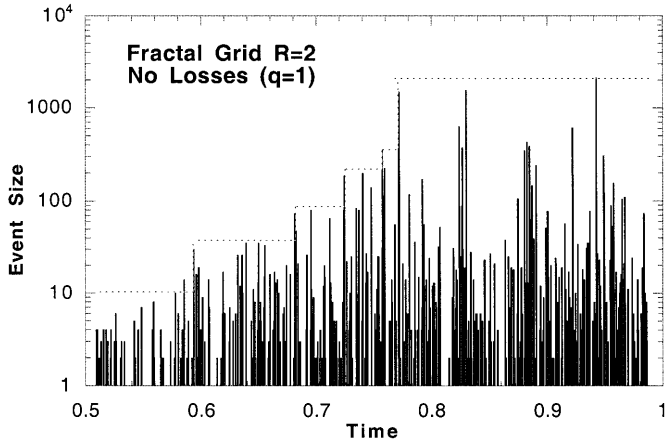

Figure 13
Seismic catalog for the $R = 2$ fractal grid with no losses illustrating the discrete jumps in event size leading up to the critical point.

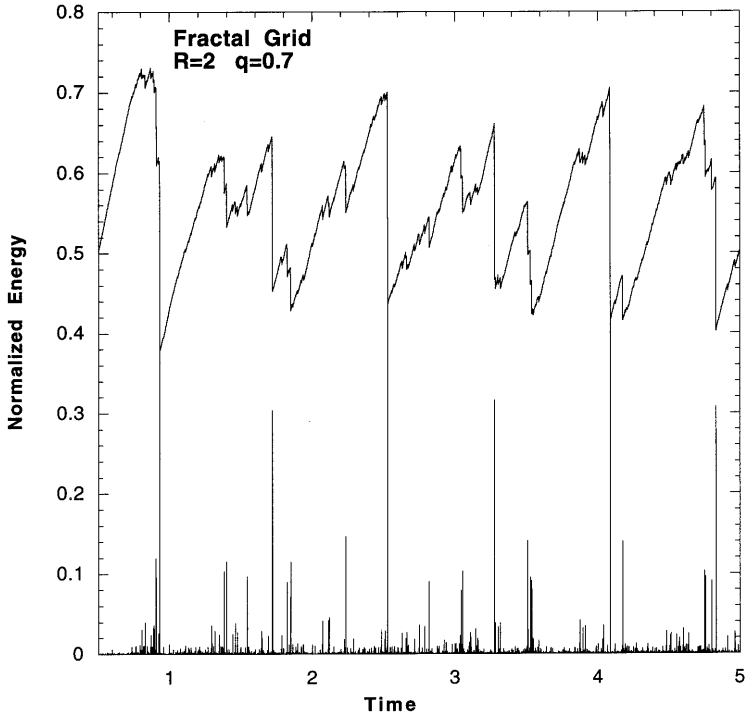

Figure 14
Energy on the grid and seismic catalog for several "cycles" of the $R = 2$ fractal automaton with $q = 0.7$. Losses appear to produce longer and more irregular cycles than in Figure 12 where $q = 1$.

The Fractal Automaton with Losses

The calculations in the previous section were repeated with $q = 0.7$ and $q = 0.5$. Figure 14 shows the catalog and scaled energy on the grid for the case $R = 2$ and $q = 0.7$. Comparison with the $q = 1$ case (Fig. 10a) shows that the effect of losses in the fractal network is to make the cycles longer and more irregular. Figure 15 shows the cumulative Benioff strain (sum of the square root of the energy of each event through time) during an initial transient approach to SOC for the $R = 2$ and $R = 3$ grids. We plot Benioff strain here because it is the quantity usually analyzed for log-periodic fluctuations (SORNETTE and SAMMIS, 1995; HUANG *et al.*, 1998). There is no theoretical reason for the choice of this parameter. Note that the wavelength of the log-periodic fluctuations is longer for the $R = 3$ case. This is the expected result based on the analysis of HUANG *et al.* (1998) since it takes longer for the correlation length to grow by a factor of 3 than by a factor of 2. However, a more definite quantitative analysis was frustrated by the large variations between different realizations of the model (probably due to the statistical nature of the log-periodic fluctuations themselves as discussed above) and by the sensitivity of the fitting procedure for the nonlinear equation (3).

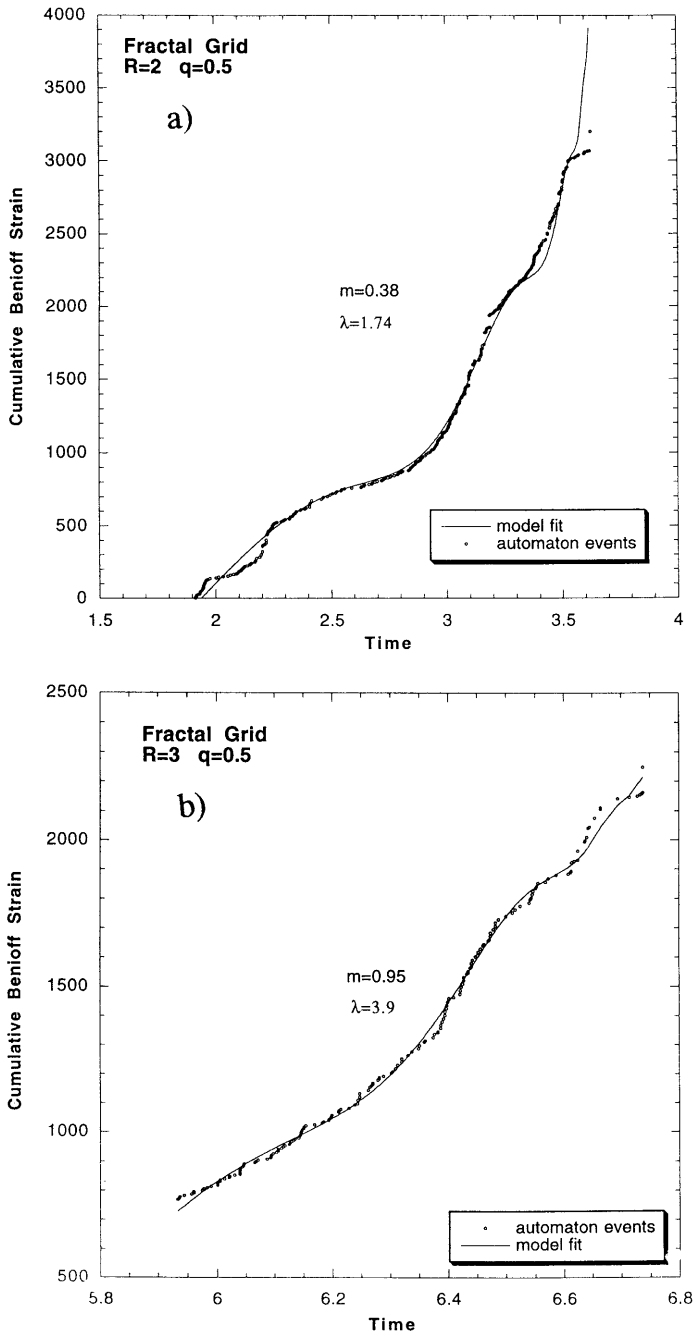

Figure 15
Cumulative Benioff strain for the fractal grids with loss factor $q = 0.5$. Note that the wavelength of the log-periodic oscillations increases with increasing R as expected.

Discussion and Conclusions

Self-organized criticality, as exhibited by the uniform cellular automaton, was proposed by BAK and TANG (1989) as a simple robust conceptual model for regional seismicity which offered an explanation for the ubiquitously observed Gutenberg–Richter power-law relation between the number of events and their energy. However, the uniform cellular automaton clearly oversimplifies the interaction between the various faults in a regional network in a number of ways. First, it considers only interactions between nearest neighbor cells while elastic interactions between faults are long-range. It also ignores time dependent effects that might arise from anelastic coupling between the crust and the mantle. Second, the cells are uniform whereas faults in natural networks are generally heterogeneous in both size and strength. Third, the only losses in the automaton are from the edges of the array whereas real earthquakes dissipate energy locally through friction, fragmentation, and elastic radiation. Fourth, a cellular automaton is usually large in comparison to the size of its individual cells so that boundary effects can be ignored. In most natural networks the size of the largest fault is a significant fraction of the size of the network.

There is mounting evidence that the spatial and temporal patterns of regional seismicity are more complicated than those predicted by the simple automaton. Other theoretical studies indicate, in contrast to the SOC paradigm, that the simulated seismicity patterns depend strongly on the assumed form of the interaction, heterogeneity, and rheology (BEN-ZION and RICE, 1995; BEN-ZION, 1996; FISHER *et al.*, 1997; DAHMEN *et al.*, 1998). In this paper we have shown that the inclusion of a local loss factor in the cascades leads to temporal cycles in the automaton seismicity which mimic many characteristics of observed seismic cycles. The largest events tend to be preceded by a power-law increase in seismicity associated with the clustering of intermediate-sized events and followed by a decrease leading to a period of relative quiescence. Even subtler characteristics of observed seismicity, such as the constant rate of small events through the cycle and the temporal clustering of larger events, are simulated by the lossy automaton. The seismic cycles associated with a local loss are a memory effect that is erased if strong random perturbations are introduced into the loading. Whether they are also destroyed by long-range interactions is an open question. We also found that the inclusion of structural heterogeneity produces similar cycles as long as the largest scale of the structure is comparable to the size of the network. Seismic cycles in lossy and structurally heterogeneous automatons are clearly seen to be associated with the repeated approach and retreat from the SOC state. The automaton allows us to document the growth in stress correlation and power-law energy increase in the scaling region near criticality and the destruction of correlation by large lossy events or by events associated with large structures and the subsequent movement of the system away from criticality.

The automatons provide other insights into spatial and temporal fluctuations in regional seismicity. For example, it is apparent that the largest event need not occur when the network reaches the critical point. At the critical point, the largest regional event is possible, but forecasting its actual occurrence becomes a nucleation problem that may ultimately limit the precision of an earthquake forecast (see also BOWMAN *et al.*, 1999). Also, although we find that log-periodic fluctuations in the power-law increase of seismicity preceding large events can result from a discrete hierarchical fractal structure, such fluctuations are statistical in nature and need not always occur.

Probably the most significant and general insight gained by this study is the central importance of the finite size of a regional seismic network in relation to the size of its largest structural element. Virtually all the details of the seismic cycle in these models are the consequence of boundary effects. The largest events in such finite networks are fundamentally different than smaller events. The power-law buildup before the largest events is uncontaminated by the seismicity associated with neighboring events, an effect which makes power-law precursors difficult to observe for smaller events. These largest events, if they are associated with a large structural element and/or they result in a significant loss of energy, move the entire system away from its critical point to produce a regional seismic cycle.

Acknowledgements

We wish to thank Bill Klein for a helpful discussion of the issue of SOC in the nonconservative automaton. This work was supported by the National Science Foundation under grant EAR-9508040.

REFERENCES

ALLÈGRE, C. J., LE MOUEL, J. L., and PROVOST, A. (1982), *Scaling Rules in Rock Fracture and Possible Implications for Earthquake Predictions*, Nature *297*, 47–49.

ALLÈGRE, C. J., and LE MOUEL, J. L. (1994), *Introduction of Scaling Technique in Brittle Failure of Rocks*, Phys. Earth Planet Inter. *87*, 85–93.

ANIFRANI, J. C., LE FLOC'H, SORNETTE, D., and SOUILLARD, B. (1995), *Universal Log-periodic Corrections to Renormalization Group Scaling for Rupture Stress Prediction from Acoustic Emissions*, J. Phys. I. France *5*, 631–638.

AVILES, C. A., SCHOLZ, C. H., and BOATWRIGHT, J. (1987), *Fractal Analysis Applied to Characteristic Segments of the San Andreas Fault*, J. Geophys. Res. *92*, 331–344.

BAK, P., TANG, C., and WIESENFELD, K. (1987), *Self-organized Criticality: An Explanation of 1/f Noise*, Phys. Rev. Lett. *59*, 381–384.

BAK, P., and TANG, C. (1989), *Earthquakes as a Self-organized Critical Phenomenon*, J. Geophys. Res. *94*, 15,635–15,637.

BARRIER, B., and TURCOTTE, D. L. (1994), *Seismicity and Self-organized Criticality*, Phys. Rev. E *49*, 1151–1160.

BEN-ZION, Y. (1996), *Stress, Slip and Earthquakes in Models of Complex Single-fault Systems Incorporating Brittle and Creep Deformations*, J. Geophys. Res. *101*, 5677–5706.

BEN-ZION, Y., and RICE, J. R. (1995), *Slip Patterns and Earthquake Populations along Different Classes of Faults in Elastic Solids*, J. Geophys. Res. *100*, 12,959–12,983.

BOWMAN, D. D., and SAMMIS, C. G. (1997), *Observational Evidence for Temporal Clustering of Intermediate-magnitude Events before Strong Earthquakes in California* (Abst.), Seismol. Res. Lett. *68*, 324.

BOWMAN, D. D., OUILLON, G., SAMMIS, C. G., SORNETTE, A., and SORNETTE, D. (1999), *An Observational Test of the Critical Earthquake Concept*, J. Geophys. Res., still in press.

BREHM, D. J., and BRAILE, L. W. (1999), *Intermediate-term Earthquake Prediction Using the Modified Time-to-failure Method in Southern California*, Bull. Seismol. Soc. Am. *89*, 275–293.

BUFE, C. G., and VARNES, D. J. (1993), *Predictive Modeling of the Seismic Cycle of the Greater San Francisco Bay Region*, J. Geophys. Res. *98*, 9871–9883.

BUFE, C. G., NISHENKO, S. P., and VARNES, D. J. (1994), *Seismicity Trends and Potential for Large Earthquakes in the Alaska–Aleutian Region*, Pure appl. geophys. *142*, 83–99.

BURRIDGE, R., and KNOPOFF, L. (1967), *Model and Theoretical Seismology*, Seis. Soc. Am. Bull. *57*, 341–371.

DAHMEN, K., ERTAS, D., and BEN-ZION, Y. (1998), *Gutenberg–Richter and Characteristic Earthquake Behavior in Simple Mean-field Models of Heterogeneous Faults*, Phys. Rev. E *58*, 1494–1501.

ELLSWORTH, W. L., LINDH, A. G., PRESCOTT, W. H., and HERD, D. J. (1981), *The 1906 San Francisco Earthquake and the Seismic Cycle*, Maurice Ewing Monogr. *4*, 126–140, Am. Geophys. Union.

FISHER, D. S., DAHMEN, K., RAMANATHAN, S., and BEN-ZION, Y. (1997), *Statistics of Earthquakes in Simple Models of Heterogeneous Faults*, Phys. Rev. Lett. *78*, 4885–4888.

GELLER, R. J., JACKSON, D. D., KAGAN, Y. Y., and MULARGIA, F. (1997), *Earthquakes Cannot Be Predicted*, Science *275*, 1616–1617.

GRASSBERGER, P. (1994), *Efficient Large-scale Simulations of a Uniformly Driven System*, Phys. Rev. E *49*, 2436–2444.

GUTENBERG, B., and RICHTER, C. F. (1956), *Magnitude and Energy of Earthquakes*, Ann. di. Geofis. *9*, 1.

HARRIS, R. A., and SIMPSON, R. W. (1996), *In the Shadow of 1857—Effect of the Great Ft. Tejon Earthquake on the Subsequent Earthquakes in Southern California*, Geophysical Res. Lett. *23*, 229–232.

HIRATA, T. (1989a), *Fractal Dimension of Fault Systems in Japan: Fractal Structure in Rock Fracture at Various Scales*, Pure appl. geophys. *131*, 157–170.

HIRATA, T. (1989b), *A Correlation between the b Value and the Fractal Dimension of Earthquakes*, J. Geophys. Res. *94*, 7507–7514.

HUANG, Y., SALEUR, H., SAMMIS, C. G., and SORNETTE, D. (1998), *Precursors, Aftershocks, Criticality and Self-organized Criticality*, Europhys. Lett. *41*, 43–48.

HUANG, Y., OUILLON, G., SALEUR, H., and SORNETTE, D. (1997), *Spontaneous Generation of Discrete Scale-invariance in Growth-models*, Phys. Rev. E *55*, 6433–6447.

JAUMÉ, S. C., and SYKES, L. R. (1999), *Evolving Toward a Critical Point: A Review of Accelerating Seismic Moment/Energy Release Prior to Large and Great Earthquakes*, Pure appl. geophys., *155*, 279–306.

JONES, L. M., and HAUKSSON, E. (1997), *The Seismic Cycle in Southern California: Precursor or Response?* Geophys. Res. Lett. *24*, 469–472.

KEYLIS-BOROK, V. I., and MALINOVSKAYA, L. N. (1964), *One Regularity in the Occurrence of Strong Earthquakes*, J. Geophys. Res. *69*, 3019–3024.

KLEIN, W., and RUNDLE, J. (1993), *Comment on "Self-organized Criticality in a Continuous, Nonconservative Cellular Automaton Modeling Earthquakes*, Phys. Rev. Lett. *71*, 1288.

KNOPOFF, L., LEVSHINA, T., KEYLIS-BOROK, V. I., and MATTONI, C. (1996), *Increased Long-range Intermediate-magnitude Earthquake Activity Prior to Strong Earthquakes in California*, J. Geophys. Res. *101*, 5779–5796.

MOREIN, G., TURCOTTE, D. L., and GABRIELOV, A. (1997), *On the Statistical Mechanics of Distributed Seismicity*, Geophys. J. Int. *131*, 552–558.

NADEAU, R. M., FOXALL, W., and MCEVILLY, T. V. (1995), *Clustering and Periodic Recurrence of Microearthquakes on the San Andreas Fault at Parkfield, California*, Science *267*, 503–507.

NAKANISHI, H., SAHIMI, M., ROBERTSON, M. C., SAMMIS, C. G., and RINTOUL, M. D. (1993), *Fractal Properties of the Distribution of Earthquake Hypocenters*, J. Phys. I France *3*, 733–739.

NEWMAN, W., GABRIELOV, A., DURAND, T., PHOENIX, S. L., and TURCOTTE, D. L. (1994), *An Exact Renormalization Model for Earthquakes and Material Failure*, *Statics and Dynamics*, Physica D *77*, 200–216.

OKUBO, P. G., and AKI, K. (1987), *Fractal Geometry in the San Andreas Fault System*, J. Geophys. Res. *92*, 345–355.

OLAMI, Z., FEDER, H. J. S., and CHRISTENSEN, K. (1992), *Self-organized Criticality in a Continuous, Nonconservative Cellular Automaton Modeling Earthquakes*, Phys. Rev. Lett. *68*, 1244–1247.

OUILLON, G., SORNETTE, D., GENTER, A., and CASTAING, C. (1996), *The Imaginary Part of Rock Jointing*, J. Phys. I France *6*, 1127–1139.

ROBERTSON, M. C., SAMMIS, C. G., SAHIMI, M., and MARTIN, A. (1995), *The 3-D Spatial Distribution of Earthquakes in Southern California with a Percolation Theory Interpretation*, J. Geophys. Res. *100*, 609–620.

RUNDLE, J. B. (1988a), *A Physical Model for Earthquakes*, *I*. J. Geophys. Res. *93*, 6237–6254.

RUNDLE, J. B. (1988b), *A Physical Model for Earthquakes*, *II*. J. Geophys. Res. *93*, 6255–6274.

RUNDLE, J. B. (1989), *A Physical Model for Earthquakes*, *II*. J. Geophys. Res. *94*, 2839–2855.

RUNDLE, J. B. (1993), *Magnitude Frequency Relations for Earthquakes Using a Statistical Mechanical Approach*, J. Geophys. Res. *98*, 21,943–21,949.

RUNDLE, J. B., KLEIN, W., and GROSS, S. (1996), *Dynamics of a Traveling Density Wave Model for Earthquakes*, Phys. Rev. Lett. *76*, 4285–4288.

RUNDLE, J. B., KLEIN, W., GROSS, S., and TURCOTTE, D. L. (1995), *Boltzmann Fluctuations in Numerical Simulations of Nonequilibrium Lattice Threshold Systems*, Phys. Rev. Lett. *76*, 1658–1661.

SAHIMI, M., ROBERTSON, M. C., and SAMMIS, C. G. (1993a), *Fractal Distribution of Earthquake Hypocenters and its Relation to Fault Patterns and Percolation*, Phys. Rev. Lett. *70*, 2186–2198.

SAHIMI, M., ROBERTSON, M. C., and SAMMIS, C. G. (1993b), *Relation between the Earthquake Statistics and Fault Patterns, and Fractals, and Percolation*, Physica A *191*, 57–68.

SAHIMI, M., and ARBABI, S. (1996), *Scaling Laws for Fracture of Heterogeneous Materials and Rock*, Phys. Rev. Lett. *77*, 3689–3692.

SALEUR, H., SAMMIS, C. G., and SORNETTE, D. (1996a), *Discrete Scale Invariance, Complex Fractal Dimensions, and Log-periodic Fluctuations in Seismicity*, J. Geophys. Res. *101*, 17,661–17,677.

SALEUR, H., SAMMIS, C. G., and SORNETTE, D. (1996b), *Renormalization Group Theory of Earthquakes*, Nonlinear Processes in Geophysics *3*, 102–109.

SAMMIS, C. G., BOWMAN, D. D., SALEUR, H., HUANG, Y., SORNETTE, D., and JOHANSEN, A. (1995), *Log-periodic Fluctuations in Regional Seismicity before and after Large Earthquakes*, EOS Trans. Am. Geophys. Union, F405.

SAMMIS, C. G., SORNETTE, D., and SALEUR, H., *Complexity and Earthquake Forecasting*, *Reduction and Predictability of Natural Disasters*, *SFI Studies in the Sciences of Complexity*, vol. XXV (eds. J. B. Rundle, W. Klein, and D. L. Turcotte) (Addison-Wesley, Reading, Mass. 1996) pp. 143–156.

SORNETTE, D., and SAMMIS, C. G. (1995), *Complex Critical Exponents from Renormalization Group Theory of Earthquakes: Implications for Earthquake Predictions*, J. Phys. I. *5*, 607–619.

SORNETTE, A., and SORNETTE, D. (1990), *Earthquake Rupture as a Critical Point: Consequences for Telluric Precursors*, Tectonophysics *179*, 327–334.

SMALLEY, R. F., TURCOTTE, D. L., and SOLLA, S. A. (1985), *A Renormalization Group Approach to the Stick-slip Behavior of Faults*, J. Geophys. Res. *90*, 1894–1900.

SYKES, L. R., and JAUMÉ, S. (1990), *Seismic Activity on Neighboring Faults as a Long-term Precursor to Large Earthquakes in the San Francisco Bay Area*, Nature *348*, 595–599.

TRIEP, E. G., and SYKES, L. R. (1997), *Frequency of Occurrence of Moderate to Great Earthquakes in Intracontinental Regions: Implications for Change in Stress, Earthquake Prediction, and Hazards Assessments*, J. Geophys. Res. *102*, 9923–9948.

VARNES, D. J., and BUFE, C. G. (1996), *The Cyclic and Fractal Seismic Series Preceding an $M_b = 4.8$ Earthquake on 1980 February 14 near the Virgin Islands*, Geophys. J. Int. *124*, 149–158.

(Received October 4, 1998, revised January 21, 1999, accepted January 22, 1999)